

AD-A114 518

FOREIGN TECHNOLOGY DIV WRIGHT-PATTERSON AFB OH

NEODYMIUM PENTAPHOSPHATE LASER, (U)

APR 82 H HE, G LU, M ZHAO, L ZHAO

UNCLASSIFIED FTD-ID(RS)T-0183-82

F/G 20/5

NL



END  
DATE  
APR 82  
6 82  
DTIC

DTIC FILE COPY

AD A114518

FTD-ID(RS)T-0183-82

(2)

## FOREIGN TECHNOLOGY DIVISION



NEODYMIUM PENTAPHOSPHATE LASER

by

He Huijuan, Lu Guoxian, et al



DTIC  
SELECTED  
MAY 17 1982  
S E

Approved for public release;  
distribution unlimited.



20 05 1982

FTD-ID(RS)T-0183-82

## EDITED TRANSLATION

FTD-ID(RS)T-0183-82

13 April 1982

MICROFICHE NR: FTD-82-C-000485

NEODYMIUM PENTAPHOSPHATE LASER

By: He Huijuan, Lu Guoxian, et al

English pages: 9

Source: Jiguang (Laser Journal), Vol. 6, Nr. 12, 1979,  
pp. 16-19

Country of origin: China

Translated by: LEO KANNER ASSOCIATES  
F33657-81-D-0264

Requester: FTD/TQID

Approved for public release; distribution unlimited.

Accession For	
NTIS GRA&I	<input checked="" type="checkbox"/>
DTIC TAB	<input type="checkbox"/>
Unannounced	<input type="checkbox"/>
Justification	
By _____	
Distribution/ _____	
Availability Codes	
Dist	Avail and/or Special

DTIC  
COPY  
INSPECTED  
2

A

THIS TRANSLATION IS A RENDITION OF THE ORIGINAL FOREIGN TEXT WITHOUT ANY ANALYTICAL OR EDITORIAL COMMENT. STATEMENTS OR THEORIES ADVOCATED OR IMPLIED ARE THOSE OF THE SOURCE AND DO NOT NECESSARILY REFLECT THE POSITION OR OPINION OF THE FOREIGN TECHNOLOGY DIVISION.

PREPARED BY:

TRANSLATION DIVISION  
FOREIGN TECHNOLOGY DIVISION  
WP-AFB, OHIO.

FTD-ID(RS)T-0183-82

Date 13 Apr 19 82

GRAPHICS DISCLAIMER

All figures, graphics, tables, equations, etc. merged into this translation were extracted from the best quality copy available.

## NEODYMIUM PENTAPHOSPHATE LASER

He Huijuan, Lu Guoxian, Zhao Meicun, and Zhao Longxin

Shanghai Institute of Optics and Fine Mechanics, Chinese Academy of Sciences

Submitted 24 April 1979

The experimental setup, test method and laser performances at room temperature for a neodymium pentaphosphate laser with a single transverse mode longitudinally pumped by a dye laser at  $0.56\mu\text{m}$  are described. The optical slope efficiency is  $\sim 10$  percent, threshold energy for single transverse mode is  $\sim 40\mu\text{J}$ . Oscillation threshold for single mode of longitudinal pumping was estimated with a simple computer model. They agree each other within the experimental error of 10 percent. A single pulse without Q-switching can be obtained by appropriately varying the cavity parameters.

### I. Foreward

Among  $\text{NdP}_5\text{O}_{14}$  crystals and other similar compounds, the concentration of  $\text{Nd}^{3+}$  is as high as  $4 \times 10^{21} \text{ cm}^{-3}$ , higher by 30 times YAG of 1-percent Nd commonly blended. In addition, the sudden extinguishing effect of  $\text{Nd}^{3+}$  concentration (in the case of  $\text{NdP}_5\text{O}_{14}$ ) is very low, therefore laser energy can be increased to a greater extent only with a very small working specimen. Thus,  $\text{NdP}_5\text{O}_{14}$  crystals can be used for miniaturization of equipment; not only can the crystal have many applications in low-power Nd:YAG laser equipment, but also it is free of those

Limitations in semiconductor laser applications because of such properties as narrow optical spectrum, good mode characteristics, and small divergence angle of light beams. For example, the  $\text{NdP}_5\text{O}_{14}$  laser is adaptable as the light source of a fiber optical communication system because of its high light-coupling efficiency and low losses in absorption and scattering. Looking forward to the development of the neodymium pentaphosphate laser, extensive applications are foreseen in communications (milliwatts to tens of milliwatts in power) between spacecraft, as light source of logics in a photon computer, and as composite laser in composite optics. Due to these above-mentioned advantages, the  $\text{NdP}_5\text{O}_{14}$  laser is highly regarded by researchers as one of the development directions of photoelectron technology.

Quite a few fraternal units are organizing the development of these compound lasers. The authors used a  $\text{NdP}_5\text{O}_{14}$  working specimen (developed by the Institute of Crystals, Shandong University) to operate at room temperature, for the first time, a single-mode  $\text{NdP}_5\text{O}_{14}$  laser of the pulse dye-laser pump.

## II. Experimental Installation and Methods

### 1. An experimental installation is shown in Fig. 1.

Rudamming [transliteration] 60 dye laser with single lens harmonic modulation by straight-tube pulse xenon lamp pump: 0.58 micron, one-half light spectrum width  $\sim 40\text{A}$ , once per second, one-half-intensity width 1 microsecond, divergence angle  $\sim 3$  milliradian.

After the pumped light passes through field aperture and two pieces of the  $45^\circ$  reflective mirror, through a focusing lens the light is concentrated on a  $\text{NdP}_5\text{O}_{14}$  lens. A 1.05-micron laser is shown on an oscilloscope through a  $45^\circ$  reflective mirror and a light filtering plate; the laser is measured by a high-current photocell or a photo-multiplier tube.

In order to achieve single-mode low-threshold-value operation considering adjustment precision, a quasi-semiconcentric cavity is used; after its polishing a 1.1-mm thick crystal plate is elastically pasted on a plane cavity plate. The light is transparent in the direction of the b axis. On a 1.05-micron plane

cavity plate, the reflectivity  $r_1=99.3$  percent and the reflectivity (of 0.58 micron)  $T_1=70$  percent; for a concave cavity plate, the radius of curvature  $\rho=60$  mm and the transparency (of 1.05 microns)  $=1.5$  percent. The cavity length and lens position can be adjusted.

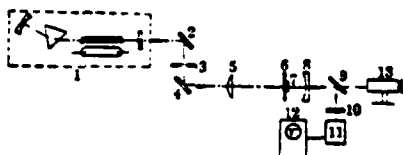


Fig. 1. Experimental installation of  $\text{NdP}_5\text{O}_{14}$  laser: 1 - dye laser of straight-tube xenon lamp pump; 2, 4 - 0.58-micron 45° reflective mirror; 3 - field aperture ( $\phi 20$ ); 5 - pumped light focusing lens,  $f=10$  cm; 6 - parallel-plane cavity plate; 7 -  $\text{NdP}_5\text{O}_{14}$  crystal; 8 - concave cavity plate; 9 - easily dismantled 1.05-micron 45° reflective mirror; 10 - 1.05-micron narrow-band interference light-filter plate and (filtering 0.58-micron color) glass plate; 11 - high-current photocell (GD-44) or photo-multiplier tube (GDB-28); 12 - pulse oscilloscope (SS-212); 13 - internal focus adjustment parallel fluorescent tube.

## 2. Experimental method

Major procedures of this experiment can be divided into three parts:

First, an internal-focus adjustable parallel fluorescent tube is used to aim the cavity straight, then an 0.58-micron laser is pumped in by adjusting two pieces of reflective mirror and focusing lens to aim the incident light with the cavity axis. Laser oscillation is achieved under the condition of a high-energy light pump as the requirement of adjustment precision of the cavity is not high. In order to achieve single-mode low-threshold-value operation, the requirement of cavity adjustment precision is high. In order to determine the

laser output of 1.05 microns, first it is to distinguish fluorescence and laser by their great differences of pulse widths between 1.05-micron fluorescence and laser. Then a monochromator (placed near a receiving element) is used to distinguish the 0.58-micron pumped light and 1.05-micron laser. In another method, the cavity length can be increased to alter it (from a metastable concentric cavity) into an unstable cavity in order to distinguish 0.58-micron pumped light from 1.05-micron laser. Generally, most laser pulse energy is measured with a brazier calorimeter; however, this type of calorimeter can only measure at the millijoule level. As the laser energy of the authors' installation is mostly at the level of microjoules to tens of microjoules, the brazier measurement method is too insensitive. After comparison and application of several methods, finally the authors decided to use a method of high-current photocell linear conversion of regional pulse integration to measure low energy levels. In this method, the aiming of the light channel is easy and the measurement precision is high when there is low environmental interference of electromagnetism with a sensitivity of microjoule level or higher. Only by varying the anode loading of high-current photocell can the pulse waveform be measured, so its operation is quite convenient.

### III. Comparison Between Experimental Results and Theoretical Calculations

1. With cavity length  $d=50.8$  mm and proper adjustment of distance between focusing lens and the crystal, the output of the 1.05-micron laser is shown in Fig. 2 as a pulse waveform. In the figure, (a) shows the laser slackening pulse (when the light pump is of relatively intensive action) composed of one main pulse and several small pulses while the attenuation time (of slackening oscillation) is approximately 2 microseconds; (b) shows a widening waveform of a single laser pulse after proper weakening of light pump. The pulse semi-intensity width is approximately 140 nanoseconds.
2. For cavity length of 59 mm and the distance between focusing lens and the crystal at 126 mm, the multi-mode laser output energy is measured by a marked high-current photocell through integration; Fig. 3 shows the light energy conversion rate relationship lines. The solid line was measured at the output terminal of the concave cavity plate; the dotted line was measured at the plane cavity plate terminal with 0.5 percent coupling output. The pumped light energy is the energy passing through the plane cavity plate and directly reaching the incident

surface of the crystal; the energy is measured with a sensitive brazier. The light energy conversion efficiency is approximately 10 percent and the photon conversion efficiency is approximately 18 percent; the results are the same as that of H. P. Weber et al [1].

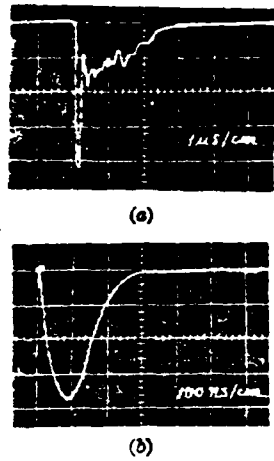


Fig. 2. Waveforms of 1.05-micron laser pulse.

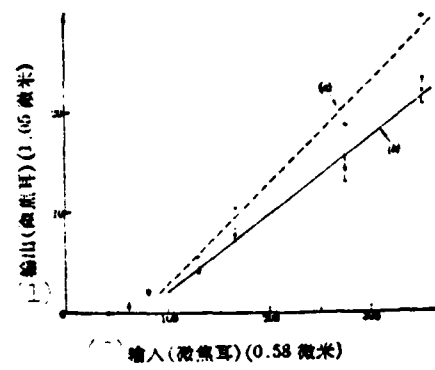


Fig. 3. Light energy conversion relationship: (a) output at both terminals; (b) output at a single terminal (actual measurement).

Key: 1. Output (microjoules);  
2. Input (microjoules) (0.58 micron).

3. For cavity length of 39 mm and the distance between focusing lens and the crystal adjusted to 122.5 mm, the near-field diagram of the maximum-dimension  $TEM_{00}$  mode of oscillation mode spot is shown in Fig. 4. At the laser output terminal, an infrared image converter tube shows the diagram with direct reception.

4. When the reflectivity  $r_2$  of output mirror is altered, the threshold value of the corresponding fundamental-mode oscillation is measured. For the threshold value  $\ln(r_1 r_2)$  curve, the cavity's noncoupling loss rate is (including crystal's resonance loss and non-resonance loss)  $\sim 2.3$  percent, as shown in Fig. 5. In the

figure, the "+" sign shows the measured value during the experiment and "o" sign shows the theoretical value as calculated through coincidence of pumped light and fundamental-mode space. The calculation formula is as follows:

$$\omega_0^2 = (\lambda/\pi) \sqrt{d(\rho-d)}^{(2)} \quad (1)$$

In Eq. (1),  $\omega_0$  is the radius (when the thickness of crystal plate is considerably smaller than the cavity length, the weak effect of the crystal thickness can be neglected) of the light spot on the crystal incident surface caused by the fundamental mode.  $\lambda$  is the oscillation wavelength,  $d$  is the geometrical length of the cavity, and  $\rho$  is the radius of curvature of the concave cavity plate.



Fig. 4.  $TEM_{00}$  field mode diagram.

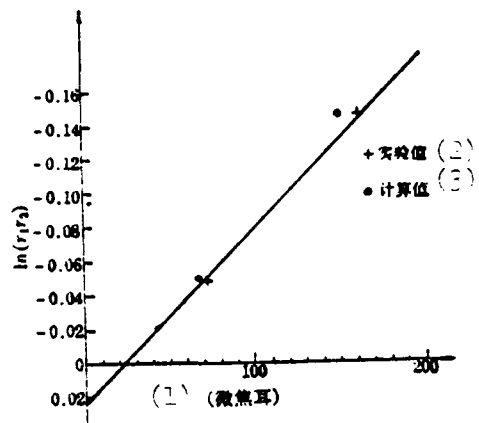


Fig. 5. Relationship between threshold value and  $\ln(r_1r_2)$ .

Key: (1) (microjoules);  
 (2) Experimental value;  
 (3) Calculation value.

When the pulse width of the pumped light is considerably smaller than the life span of  $Nd^{3+}$  fluorescence, starting from the feedback and negative feedback model of micro-disturbance of spontaneous radiation, the density of the energy plane of the laser pulse oscillation threshold value is

$$E_n = \hbar c L_c \times 10^{-3} / 2\lambda_p \alpha_p \sigma F \eta^{(3)} \quad (2)$$

In the equation,  $L_c$  is the total laser loss-rate after a round trip in the cavity;  $\lambda_p$  is the pump wavelength;  $\alpha_p$  is the absorption rate of pumped light by the laser

working spectrum;  $F$  is the percentage of the  $\text{Nd}^{3+}$  particles at the  $4F_{3/2}$  state laser energy level;  $\eta$  is the conversion efficiency when the pump photon enters the  $4F_{3/2}$  state;  $\sigma$  is the excited emitting cross-section at 1.05 microns by  $\text{Nd}^{3+}$ ;  $h$  is the Planck's constant; and  $c$  is the speed of light.

As calculated from Equations (1) and (2), the theoretical and experimental values are listed in Table 1. From the table, these two values are more-or-less matching for the approximate model and error range.

## II. Conclusions

1. From the relatively good matching between the experimental values and theoretical calculation values of threshold-value energy of the fundamental mode, it is proved to be feasible to use the longitudinal-direction pump as a simple calculation model. Without more improved conditions of the experimental precision and error, more precise calculation models are not necessary. From actual measurements, the noncoupling loss of the cavity is as high as 2.3 percent. This explains that only with further improvement in the quality of crystal optics, higher reflectivity by using vacuum coated film, and higher precision of the cavity plate adjustment frame, can even lower threshold-value oscillation energy be obtained.
2. Varieties of longitudinal-direction pump can conveniently carry out mode control and, in addition, mode modulation can be executed. In some particular application case, perhaps the properties of laser mode modulation can be utilized. The mode varieties are shown in Fig. 6.
3. By proper control of light pump energy, single pulse operation can be conveniently carry out. If properly changing the parameters of the harmonic oscillation cavity (such as cavity length and loss), it is anticipated that within a certain pulse-width range, an adjustable laser single pulse (with  $Q$  switch) may be obtained.

Table 1. Calculated and experimental values of threshold energy value.

(a) $\lambda$ (厘米)	$1.05 \times 10^{-4}$	$1.05 \times 10^{-4}$	$1.05 \times 10^{-4}$
(a) $\lambda_p$ (厘米)	$0.58 \times 10^{-4}$	$0.58 \times 10^{-4}$	$0.85 \times 10^{-4}$
$a_p$ (%)	100	100	100
$F$ (%)	63	63	63
(b) $\sigma$ (厘米 $^2$ )	$1.8 \times 10^{-19}$	$1.8 \times 10^{-19}$	$1.8 \times 10^{-19}$
$\eta$ (%)	60	60	60
(a) $d$ (厘米)	3.9	3.9	3.9
(a) $\rho$ (厘米)	6.0	6.0	6.0
(a) $w_0$ (厘米)	$9.83 \times 10^{-3}$	$9.83 \times 10^{-3}$	$9.83 \times 10^{-3}$
(b) $\pi w_0^2$ (厘米 $^2$ )	$3.04 \times 10^{-4}$	$3.04 \times 10^{-4}$	$3.04 \times 10^{-4}$
$r_1$ (%)	99.3	99.3	99.3
$r_2$ (%)	98.5	95.8	87
$\ln r_1 r_2$	-0.022	-0.049	-0.146
$L_t$ (%)	$2.3+0.7$ $+1.5=4.5$	$2.3+0.7$ $+4.2=7.2$	$2.3+0.7$ $+13=16$
(c) $E_{th}$ (微焦耳/厘米 $^2$ )	$1.4 \times 10^6$	$2.23 \times 10^6$	$5 \times 10^6$
(d) $E_{th,exp}$ (微焦耳)	42	67	150
(d) $E_{th,cal}$ (e) (微焦耳)	42	72	162

Key: (a) (centimeters); (b) (square centimeters); (c) (microjoules per square centimeter); (d) (microjoules); (e)  $E_{th}$  experiment.

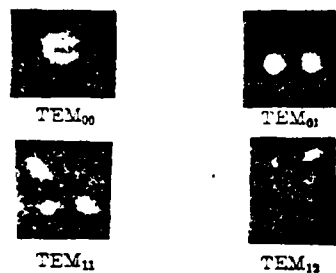


Fig. 6. Laser modes manifested by adjusting positions of focusing lens.

#### LITERATURE

1. APPL. PHYS. LETT., 22, 534 (1973).
2. APPL. OPT., 5, 1557 (1966).
3. J. APPL. PHYS., 46, 1194 (1975).

END

DATE  
FILMED

6-82

DTIC